A Custom Analysis of RR Interval Properties Reveals Alterations of the Brain-Heart Axis in Experimental Animals with Metabolic Syndrome

Olivier Meste, Michael Sun, Daniel Cervantes, Giulia Piccinini, Bob Qian, Zoë Volney, Belinda Nyantakyi, Georgette Cosentino, Aaron Yancoskie, Sudhir Jain, et al.

A custom analysis of R-R interval properties reveals alterations in the brain-heart axis in experimental animals with metabolic syndrome

Olivier Meste, PhD,[1,7] Michael Y. Sun, BS,[2,7] Daniel O. Cervantes, MD,[2,7] Giulia Piccinini, MS,[2] Bob Qian, BS,[2] Zoë Volney, BS,[2] Belinda Nyantakyi, MS,[2] Georgette A. Cosentino, BS,[2] Aaron Yancoskie, DDS,[3] Sudhir Jain, PhD,[4] Jason T. Jacobson, MD,[2,5] Malik Bisserier, PhD,[2,6] Marcello Rota, PhD[2]

From the [1]Université Côte d'Azur, CNRS, I3S, Sophia Antipolis, France, [2]Department of Physiology, New York Medical College, Valhalla, New York, [3]Touro College of Dental Medicine, Valhalla, New York, [4]Department of Pathology, Microbiology and Immunology, New York Medical College, Valhalla, New York, [5]Division of Cardiology, Westchester Medical Center, Valhalla, New York, and [6]Department of Cell Biology and Anatomy, New York Medical College, Valhalla, New York.

BACKGROUND Metabolic syndrome (MetS) is a cluster of conditions that increases the risk of cardiovascular complications and all-cause mortality. MetS manifests reduced heart rate variability, but factors underlying the process remain to be fully elucidated.

OBJECTIVE To gain new insights into the effects of MetS on heart rhythm dynamics, we developed a custom algorithm to analyze the distribution and span of R-R intervals.

METHODS MetS was induced in male and female mice by Western diet feeding (WD mice), whereas animals on regular chow were used as controls (Ctrl mice). The sequence of R-R intervals of electrocardiograms and their deviation were sorted and normalized using an approximation of the distribution function to obtain sequences of the R-R interval duration (sortRR) and the R-R interval deviation (sortRRdev).

RESULTS sortRR sequences revealed shorter intervals in WD mice than in Ctrl mice within the range of intermediate and long R-R intervals, indicating that mice with MetS have limited capability to lower heart rate. Moreover, sortRRdev sequences had smaller amplitudes for WD mice, consistent with reduced heart rate variability. Inhibition of sympathetic inputs abrogated differences in sortRR sequences for the 2 groups of mice, whereas inhibition of parasympathetic inputs suppressed differences in the sortRRdev series. Interestingly, Western diet feeding in animals lacking β-adrenergic receptors minimally affected heart rate dynamics in female mice, but revealed significant alterations in male animals, which were abrogated by parasympathetic inhibition.

CONCLUSION These results support the notion that sympathoexcitation and parasympathetic withdrawal occur with MetS and affect the duration, functional range, and variability of R-R intervals.

KEYWORDS Metabolic syndrome; Heart rate variability; Sympathovagal balance; Brain-heart axis; R-R interval

(Heart Rhythm O^2 2025;■:1–18)

Introduction

Metabolic syndrome (MetS) is a multicomponent risk factor for cardiovascular disease and diabetes and is associated with the clustering of abnormalities related to abdominal obesity, insulin resistance, hypertension, and dyslipidemia.[1,2] MetS is becoming highly prevalent and affects approximately one-third of the male and female adult population worldwide,[1] representing a significant and growing public health problem.

MetS manifests preclinical diastolic dysfunction alone or in combination with left ventricular (LV) hypertrophy, which are important risks for the development of heart failure with preserved ejection fraction (HFpEF).[3–5] Interestingly, altered cardiac autonomic regulation anticipates the functional and structural remodeling of the LV in patients with metabolic disorders,[6–8] and it gradually worsens with the number of risk components for MetS.[9–11] Autonomic imbalance contributes to exercise intolerance[12] and constitutes, per se, an additional and independent risk variable for heart failure, arrhythmias, and mortality,[13–15] constituting a critical component of the cardiometabolic syndrome.

[7]Dr Meste, Mr Sun, and Dr Cervantes contributed equally to this work. **Address reprint requests and correspondence:** Dr Marcello Rota, Department of Physiology, New York Medical College, Room 617, Basic Science Bldg, 15 Dana Rd, Valhalla, NY 10595. E-mail address: marcello_rota@nymc.edu.

2666-5018/

https://doi.org/10.1016/j.hroo.2025.11.025

KEY FINDINGS

- Sympathoexcitation and withdrawal of parasympathetic tone occur in metabolic syndrome, affecting heart rate dynamics.
- Metabolic syndrome constrains the functional range of heart rate and impairs the heart's ability to adapt to low beating frequencies.
- The sortRR (percentile distribution of R-R interval durations) analytical approach provides novel quantitative and graphical representations of heart rate variability distribution that are not captured by traditional metrics.
- The sortRR framework defines R-R interval ranges influenced by pathological conditions or pharmacological interventions, underscoring its potential as an investigative tool for basic cardiovascular research and clinical screening.

The sympathetic and parasympathetic branches of the autonomic nervous system innervate the sinoatrial node and regulate heart rate by modulating diastolic depolarization of the pacemaker cells.[16–19] Based on the antagonistic effects and modality of action of the 2 branches of the autonomic system on sinoatrial node discharge, the analysis of heart rate variability (HRV) provides information on the influence of sympathetic and parasympathetic inputs on the heart.[20–22] Specifically, by measuring intervals between consecutive R waves of the electrocardiogram (ECG), short-term (ie, beat-to-beat) variations, long-term changes, as well as fluctuation patterns of R-R interval duration are assessed using time-domain, frequency-domain, and nonlinear metrics.[21–23] But parameters directed to the assessment of the distribution of R-R intervals and range of heart rate function are not commonly used. Therefore, to fill this gap, we have developed a custom algorithm for the quantification and graphical representation of R-R interval distribution for experimental subjects. Specifically, R-R intervals obtained from ECGs collected from conscious mice were sorted and expressed using a percentile function, and the distribution of R-R interval durations was then used for quantification and statistical comparison.

In the present study, using conventional HRV analysis and our custom analytical approach, we have evaluated the consequences of diet-induced MetS on heart rhythm dynamics in male and female mice. Using pharmacological interventions and engineered mice lacking β-adrenergic receptors (β-ARs), we provide documentation of the central role of the cardiac autonomic nervous system in the manifestations of MetS, as well as the relative contribution of sympathetic and parasympathetic defects to alterations in heart rate dynamics.

Methods

All data, materials, and methods of this study are available from the corresponding author upon reasonable request.

Large language models were not used for manuscript creation and/or drafting.

Animals

The research reported in this article adhered to Animal Research: Reporting of In Vivo Experiments guidelines and the *Guide for the Care and Use of Laboratory Animals*. Animal housing and experiments were approved by the local animal care committees (Institutional Animal Care and Use Committee) of New York Medical College.

Female and male C57Bl/6 mice (n = 50 for each sex) were obtained from Charles River Laboratories (Wilmington, MA). Mice were kept on a 12-hour light/dark cycle with water and food ad libitum. Cohorts of animals were fed regular chow (Laboratory Rodent Diet 5001, LabDiet, containing 13.6% fat of total calories and 0.4% sodium) and assigned to the control group (Ctrl mice) or maintained on a Western diet (D12079B, Research Diets, containing 40.3% fat of total calories, supplemented with 2% sodium chloride) starting at 2–3 months of age and assigned to the Western diet group (WD mice) to induce manifestations consistent with MetS.[24–26] The Western diet used here was previously reported to increase serum levels of nonesterified fatty acids and total cholesterol in mice.[24] In vivo measurements were performed during the light cycle.

Mice lacking β1- and β2-ARs (β-AR global knockout mice [BAR-KO mice]),[27] originally obtained from the Jackson Laboratory (STOCK Adrb1^{tm1Bkk} Adrb2^{tm1Bkk}/J; strain: 003810) were also used in this study. A total of 30 male and 32 female BAR-KO mice were used in this investigation. Cohorts of BAR-KO mice were fed regular chow or Western diet. Bar graphs for data related to BAR-KO mice are shown with solid pink colors in the graphical representations.

For tests addressing the effects of Western diet, 20 male and 20 female C57Bl/6 mice and 13 male and 10 female BAR-KO mice were fed the Western diet. A total of 20 male and 20 female C57Bl/6 mice and 10 male and 13 female BAR-KO mice were fed regular chow and used as controls for comparison with the Western diet group.

ECG recordings

To record ECGs in conscious animals, an ECG-tunnel device (emka Technologies) was used.[22,28,29] Animals were placed in a tunnel, and ECGs were recorded for a period of 10 minutes, unless otherwise specified. Electrode cream (SignaCreme, ParkerLabs) was placed on the mouse paws to improve the quality of electrical signals. Electrical signals were amplified with a 12-lead ECG amplifier (Ponemah Software, DSI), digitized using a 160-kHz A/D converter (DI-1120 HS, DATAQ Instruments), and recorded with WinDaq software (DATAQ Instruments) at a 10-kHz sampling rate. The bipolar leads I, II, and III and the unipolar lead aVL were

collected. Electrical signals were evaluated offline with LabChart 8 (ADInstruments).[22,28–30]

Effects of pharmacological compounds on heart rate were tested by acquiring ECGs after drug administration. To interfere with the autonomic nervous system, mice were administered with atropine (MilliporeSigma, 0.5 mg/kg body weight [BW], intraperitoneally [i.p.]) for parasympathetic blockade, propranolol (MilliporeSigma, 1 mg/kg BW, i.p.) for sympathetic blockade, or the combination of atropine (0.5 mg/kg BW, i.p.) and propranolol (1 mg/kg BW, i.p.) for the combined block of sympathetic and parasympathetic branches of the autonomic nervous system (combined autonomic block [CAB]).[21,31,32] Phenylephrine (MilliporeSigma, 3 mg/kg BW, i.p.) was used to induce vasoconstriction and elevation of blood pressure to activate the baroreceptor reflex.[33,34] Blood pressure was not monitored after administration of phenylephrine. Drugs were dissolved in United States Pharmacopeia saline solution. Effects of parasympathetic, sympathetic, or combined autonomic block were evaluated at ~10 minutes after drug(s) administration, unless otherwise specified. Timing of acquisition and dosages of atropine and propranolol are similar to those previously used in mice by us[22,31,32] or by other groups.[33,35–37]

Analysis of HRV with standard metrics

Analysis of HRV was performed on ECG recordings using LabChart 8 and the HRV module, as previously reported.[21,22,26] Lead I was used to obtain HRV parameters, and other leads were used as alternative source of analysis and/or for validation of obtained results. The entire 10 minutes of ECG recording was analyzed. Company presets of the LabChart HRV module for the mouse were adopted, with minor modifications of parameters for beat classification to exclude signal artifacts. The software automatically excluded ectopic beats from the analysis, and the operator visually confirmed the accuracy of this exclusion. Parameters of HRV were generated by the software, and values were exported to Microsoft Excel for quantification.

The average duration of R-R intervals (average R-R interval duration) was evaluated over the 10 minutes of acquisition. Rhythm variability was measured using time-domain, frequency-domain, and nonlinear variables.[20–23,33] Specifically, time-domain metrics included standard deviation of R-R intervals (SDRR) and square root of the mean of the squared differences between adjacent R-R intervals (RMSSD; an index of short-term variability). Frequency-domain variables included total power of R-R interval variation (milliseconds squared), corresponding to energy in the entire power spectrum analyzed (0–5 Hz). The spectrum of oscillations of the R-R interval duration was separated into very low-frequency power (between 0 and 0.15 Hz), low-frequency (LF) power (between 0.15 and 1.5 Hz), and high-frequency (HF) power (between 1.5 and 5 Hz). Moreover, the LF/HF ratio (milliseconds squared/milliseconds squared) was computed. As previously reported,[21,22,26] HF components of R-R interval variations are attributed to respiratory-mediated modulation of R-R intervals by the parasympathetic system, whereas LF components are ascribed to baroreflex-mediated modulation of heart rate.[20,22,23] Very low-frequency components of R-R interval variation are attributed to the regulatory action of the renin-angiotensin system, thermoregulation, and, partly, parasympathetic tone.[22,23] LF components are influenced by both the sympathetic and parasympathetic axes,[20] and the LF/HF ratio is generally accepted as an index of sympathovagal balance, estimating the ratio of sympathetic to vagus nerve tone.[20,23] Nonlinear parameters were obtained from data of Poincaré plots, a graphical representation of R-R interval (RR_n) plotted against the next one (RR_{n+1}).[21,22] Specifically, the standard deviation of instantaneous beat-to-beat interval variability (SD1) and the standard deviation of continuous long-term R-R interval variability (SD2) were obtained by the ellipse-fitting technique of data plotted in Poincaré plots. The SD1 index correlates with the short-term (beat-to-beat) variability of R-R intervals and is mainly influenced by parasympathetic modulation, whereas SD2 measures the long-term variability of R-R intervals and reflects, in part, sympathetic activation.[21,22,38] Thus, the SD1/SD2 ratio is an index of autonomic balance, and it inversely correlates with the LF/HF ratio.[21–23]

A nonlinear approach based on sample entropy (SampEn) was introduced as complexity measure[39,40] of R-R intervals. SampEn was calculated using a custom-written MATLAB script obtained from MATLAB File Exchange repository (code available at https://www.mathworks.com/matlabcentral/fileexchange/124326-sampen; MATLAB Central File Exchange).[40] Setting adapted to HRV analysis were used (tolerance, $r = 0.2$ and embedding dimention, $m = 2$).

For classical HRV metrics, data are presented as medians and interquartile ranges with dot plots. Fold and percentage changes are referred to the median values. Statistical analysis was performed using Prism 10 (GraphPad). Data were initially tested for normality (Shapiro-Wilk test) and equal variance to determine the appropriate parametric or nonparametric analysis. The Student *t* test or Mann-Whitney *U* test was used for comparison between the 2 groups.[29–31,41,42] For comparison of data involving 2 factors (ie, diet and pharmacological interventions), 2-way analysis of variance followed by an uncorrected Fisher least significant difference test for multiple comparisons.[29] $P < .05$ was considered significant. Unless otherwise specified, asterisks are used in graphical representations to denote *P* values: $*P < .05$, $**P < .01$, $***P < .001$, and $****P < .0001$.

Analysis of HRV with a custom algorithm

To obtain information on the span and distribution of R-R interval durations in experimental subjects, an approximation of the distribution function of R-R intervals was implemented. Specifically, a custom algorithm for the measurement of the R-R interval duration for ECGs collected over a period of 10 minutes was developed using MATLAB

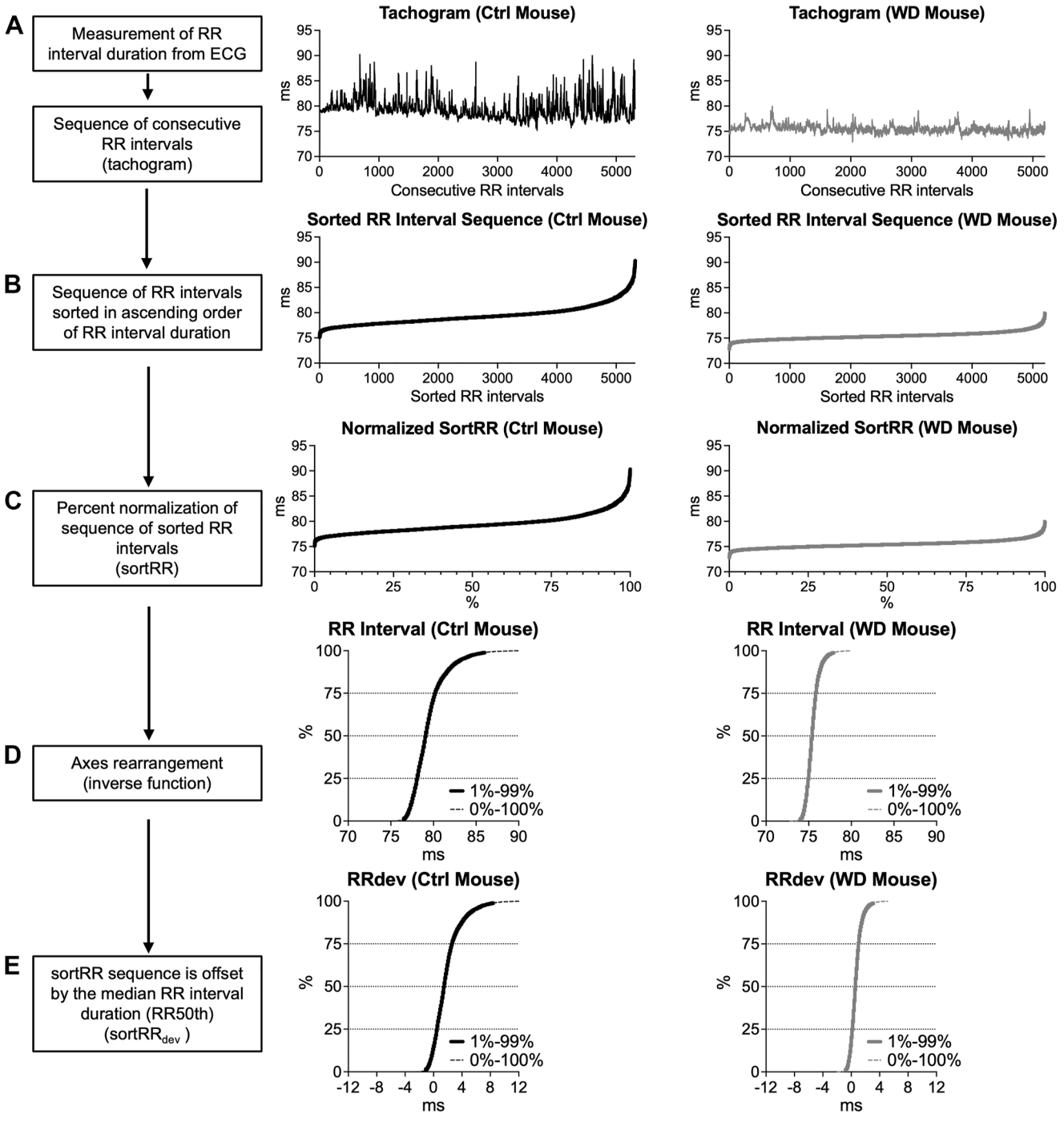

Figure 1 Flowchart of the custom algorithm for R-R interval processing. Block diagram and graphical outputs of R-R interval processing from electrocardiographic (ECG) recordings obtained from a control (Ctrl) mouse (left panels) and a Western diet (WD)–fed mouse (right panels) are reported. **A:** For each recording, the sequence of consecutive R-R intervals (tachogram) reporting R-R interval duration (y-axis) for consecutive beats (x-axis) was obtained from the ECG recording lasting for 10 minutes. A total of 5320 heartbeats were collected from the Ctrl mouse (left panel) and 5201 heartbeats were collected from the WD mouse (right panel). **B:** R-R intervals were sorted in ascending order on the basis of the R-R interval duration. **C:** The sorted sequences of R-R intervals were normalized using a percentile function. **D:** Representation of R-R interval sequences (sortRR) reporting R-R interval duration on the x-axis and percentile on the y-axis. **E:** Representations of deviations of R-R intervals from their median value (RRdev) sequences (sortRRdev) were obtained by subtracting the median of the R-R interval duration (RR_{50th}) from the sortRR sequence (sortRRdev = sortRR – RR_{50th}). In panels D and E, curves for the entire sequence (0%–100%, *dashed line*) and for the sequence omitting the 1st and 100th percentiles (1%–99%) are shown. The *horizontal dotted lines* identify the 1st quartile (25th percentile), the 2nd quartile (median, 50th percentile), and the 3rd quartile (75th percentile).

(MathWorks). Ectopic beats and artifactual peaks were rejected by the algorithm based on QRS morphology comparison (Supplemental Figure 1). Moreover, R-R interval values were filtered using a median-based threshold and outlier values were excluded from the analysis. The accuracy of R-R interval detection was confirmed through visual inspection. The sequence of consecutive R-R intervals for each recording (Figure 1A) was sorted in ascending order based on R-R interval duration to obtain the cumulative distribution function of R-R intervals (Figure 1B). Subsequently, the total number of R-R intervals of the sorted sequence was normalized using a percentile function to obtain the percentile distribution of R-R interval durations (sortRR) (Figure 1C). The sortRR sequence was graphically represented with percentile on the x-axis and duration of R-R intervals on the y-axis (Figure 1D). The sortRR sequence consisted of 2000 data points with 0.05th percentile resolution.

To obtain information on R-R interval variation, deviations of R-R intervals from their median value (RRdev) were computed for each ECG recording. Specifically, the sortRR sequence was offset with respect to the median R-R interval value (RR_{50th}) of the series to obtain the sortRRdev sequence (sortRRdev = sortRR – RR_{50th}) (Figure 1E).

To evaluate short-term (beat-to-beat) variability, values corresponding to the difference in consecutive R-R intervals for each recording were computed ($\Delta RR = RR_{n+1} - RR_n$) (Supplemental Figure 2A), as done for the calculation of RMSSD. The sequence of consecutive ΔRR intervals for each recording was then sorted in ascending order (Supplemental Figure 2B). Subsequently, the total number of beats of the sorted sequence was normalized using a percentile function to obtain the percentile distribution of ΔRR intervals (sortΔRR) (Supplemental Figure 2C). The sortΔRR sequence was graphically represented with percentile on the x-axis and duration of ΔRR intervals on the y-axis (Supplemental Figure 2D).

For quantitative data, sorted and normalized sequences for various subjects were combined to generate aggregate series for each group. Median ± median absolute deviation was used to represent the cumulative distribution plot in the 1%–99% range of the sorted sequence. The 1st and 100th percentiles were omitted from the graphical representation to minimize the inclusion of outlier values in sorted plots and to facilitate the visualization of the data set distribution. This approach was used to represent sortRR, sortRRdev, and sortΔRR.

To evaluate the suitability of the custom algorithm to assess heart rhythm dynamics in human subjects, initial tests were performed using publicly available ECGs from the database "Autonomic Aging: A dataset to quantify changes of cardiovascular autonomic function during healthy aging" deposited on PhysioNet.[43–45]

For statistical comparison of sorted sequences, an approach based on the shift function[46] was applied. Specifically, statistical differences between 2 sorted sequences were computed at each exact percentile level using a Mann-Whitney U test. Multiple-comparison corrections were applied to limit false-positive findings: the Benjamini-Hochberg[47] procedure controlled the false discovery rate, whereas the Max-T correction[48] controlled the family-wise error rate, that is, the probability of any false positive across all tests. These tests were applied globally across the 100 P values obtained at exact percentile levels of the sorted sequences. For statistical comparison, the interpolation of data points at exact percentiles levels allowed the preservation of sample size and statistical power throughout the sequence. Significance was assumed when either the Benjamini-Hochberg procedure– or Max-T correction–adjusted P values were below .05.

The MATLAB codes used for R-R interval detection and sortRR analysis in the present investigation are publicly accessible at https://figshare.com/s/9c037d8c6732acd53e4f.

Results

MetS alters heart rate dynamics in rodents

To obtain information on the consequences of MetS on the regulation of the heart by the autonomic nervous system, heart rate dynamics were evaluated in female and male C57Bl/6 mice fed the Western diet for ∼4 months, a dietary paradigm that induces metabolic disorders in rodents.[26] Animals fed the Western diet are referred to as WD mice. Age-matched mice fed regular chow were used as controls and identified as Ctrl mice. HRV parameters were computed using ECGs collected from conscious, restrained mice for 10 minutes by using a tunnel device.[21,22] Initially, R-R intervals of the ECG were analyzed using time-domain, frequency-domain, and nonlinear approaches, which provide standard metrics of HRV.[21–23]

Compared with Ctrl female mice, WD female animals presented a 2% shorter average R-R interval duration and a 47% reduction in SDRR, an index of long-term variability (Figure 2A–2C). In contrast, RMSSD, an index of short-term variability, and the total power associated with R-R interval oscillations were not significantly altered by the Western diet in female mice. Parameters of nonlinear analysis based on Poincaré plots mirrored the results of time-domain examination (Supplemental Figure 3A).

Similarly, WD male animals had reduced SDRR compared with Ctrl mice, together with attenuation of RMSSD (−24%), total power of R-R interval oscillations (−77%), and nonlinear indices of short- and long-term variability (Figure 2D and Supplemental Figure 3B). When comparing the 2 sexes, no major differences were observed between male and female mice on the regular diet. However, for WD animals, the short-term variability parameters RMSSD and SD1 and total power of R-R interval oscillations were, respectively, 21%, 21%, and 46% smaller in male mice than in female mice (Supplemental Figure 3C).

Collectively, the evaluation of HRV using classical analysis indicates that MetS reduces long-term R-R interval variability in female mice and both long-term and short-term R-R interval variability in male animals. These findings

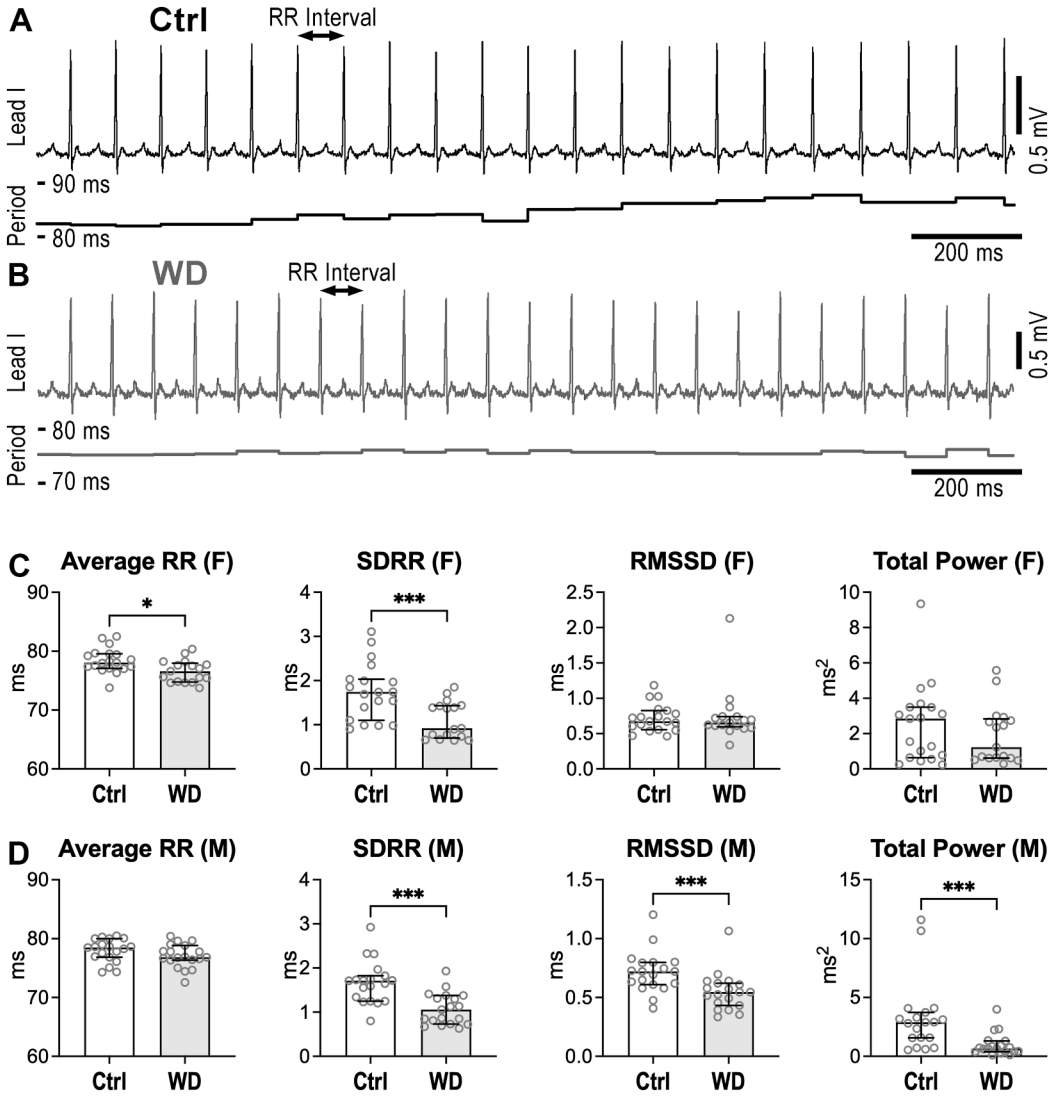

Figure 2 Western diet alters heart rhythm dynamics. **A and B:** ECG traces (Lead I) and R-R interval duration (Period) obtained in a control (Ctrl) female mouse (panel A) and a Western diet (WD)–fed female mouse (panel B). Representative intervals between consecutive R waves for each trace are reported. **C:** Quantitative data for average R-R interval duration, standard deviation of R-R interval durations (SDRR), square root of the mean of the squared differences between adjacent R-R intervals (RMSSD), and total power or oscillations of the R-R interval duration obtained by frequency-domain analysis in Ctrl mice (n = 19) and WD mice (n = 17). **D:** Quantitative data for Ctrl male mice (n = 19) and WD male mice (n = 19). Data are presented as medians and interquartile ranges (IQRs) with dot plots. *$P < .05$ and ***$P < .001$ using an unpaired *t* test or a Mann-Whitney *U* test. Similar tests are applied in subsequent figures. F = female mouse; M = male mouse.

are consistent with the notion that MetS is associated with sympathoexcitation and, at least in male animals, parasympathetic withdrawal.

MetS alters the span, distribution, and variation of R-R intervals in rodents

To obtain additional information on the effects of the Western diet on heart rhythm dynamics, a custom algorithm was used to evaluate the span and distribution of R-R interval features from ECG recordings collected from Ctrl and WD mice. Specifically, R-R intervals for the 2 groups of mice were processed to obtain the distribution of R-R intervals, allowing profile comparison (see Methods and Figure 1).

In female animals, the R-R interval duration spanned from ~75 to 85 ms (~9.6 ms span) in Ctrl mice and from ~75 to 80 ms (~5.2 ms span) in WD animals (Figure 3A). The shift function, which was used to compare and visualize the difference in R-R interval duration at each percentile level, revealed that R-R intervals were significantly shorter in WD mice for ranges corresponding to intermediate and low heart rates.

To evaluate the effects of MetS on R-R interval variation, deviations of R-R intervals from their median value were obtained using sortRRdev sequences (sortRRdev = sortRR – RR_{50th}) (see Figure 1E). For female animals, RRdev varied from −2.4 to +5.4 ms in Ctrl mice and from −1.7 to +2.5 ms in WD animals (Figure 3B). Overall, absolute values of RRdev were significantly smaller in WD mice than in Ctrl animals, indicating that animals on the Western diet had attenuated R-R interval variability.

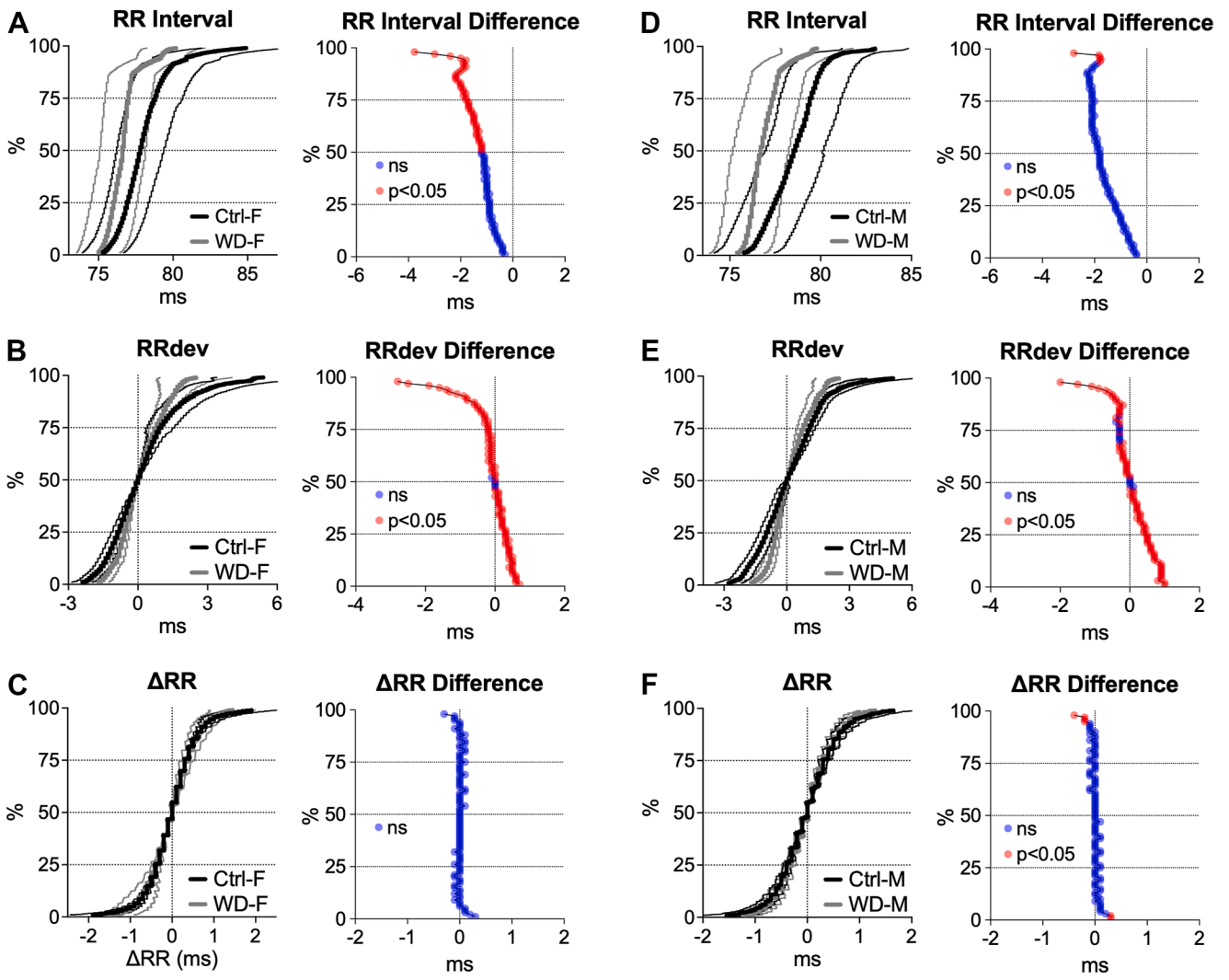

Figure 3 Western diet alters the span, distribution, and variation of R-R interval durations in male and female mice. Quantitative data for R-R interval properties for Ctrl female mice (n = 19) and WD female mice (n = 17). **A:** Aggregate data for sortRR sequences for Ctrl (Ctrl-F, *black lines*) and WD (WD-F, *gray lines*) mice are presented as median ± median absolute deviation (MAD) (left panel). The right panel illustrates the shift function showing differences and statistical significance of R-R interval duration between WD and Ctrl mice at each exact percentile. Statistical comparisons were performed using the Mann-Whitney *U* test at each percentile, followed by a multiple-comparison correction (see Methods). Significant *P* values (<.05) are indicated by *red dots*, whereas nonsignificant ($P \geq .05$) differences are indicated by *blue dots*. Similar tests were applied to data sets shown in other panels and figures. **B:** Aggregate data for sortRRdev sequences (left panel) for Ctrl and WD mice are presented as median ± MAD. The right panel reports the shift function with differences in RRdev between WD and Ctrl mice at each percentile level. **C:** Aggregate data for sortΔRR (percentile distribution of ΔRR intervals) sequences (left panel) for Ctrl and WD mice are presented as median ± MAD. The right panel reports the shift function with differences in ΔRR (difference in consecutive R-R intervals for each recording) between WD and Ctrl mice at each percentile level. **D–F:** Quantitative data for R-R interval duration properties for Ctrl male mice (n = 19) and WD male mice (n = 19). Aggregate data for sortRR (panel D), sortRRdev (panel E), and sortΔRR (panel F) sequences and corresponding shift functions for Ctrl and WD mice are presented. Abbreviations as in Figures 1 and 2.

To establish the consequences of MetS on the span and distribution of short-term variability, the difference in consecutive R-R intervals for each recording was computed ($\Delta RR = RR_{n+1} - RR_n$). Obtained values were sorted to generate ΔRR sequences (sortΔRR) (see Methods and Supplemental Figure 2). For the female sex, ΔRR was similar between Ctrl and WD mice (Figure 3C).

For male mice, using distribution profiles, R-R intervals were comparable between Ctrl and WD animals except for long R-R interval durations, corresponding to low heart rates, where the R-R interval was shorter in WD mice (Figure 3D). As observed in female animals, the absolute values of the sortRRdev sequences, reporting the variation of R-R intervals with respect to their media value, were significantly smaller in WD male mice than in Ctrl male animals (Figure 3E). Moreover, absolute values of ΔRR were reduced in WD mice at the positive and negative extremes of the sortΔRR sequences (Figure 3F), corresponding to the largest beat-to-beat variations for the 2 groups.

When comparing male and female animals, no differences between the 2 sexes were observed under the 2 dietary conditions with respect to sortRR, sortRRdev, and sortΔRR sequences.

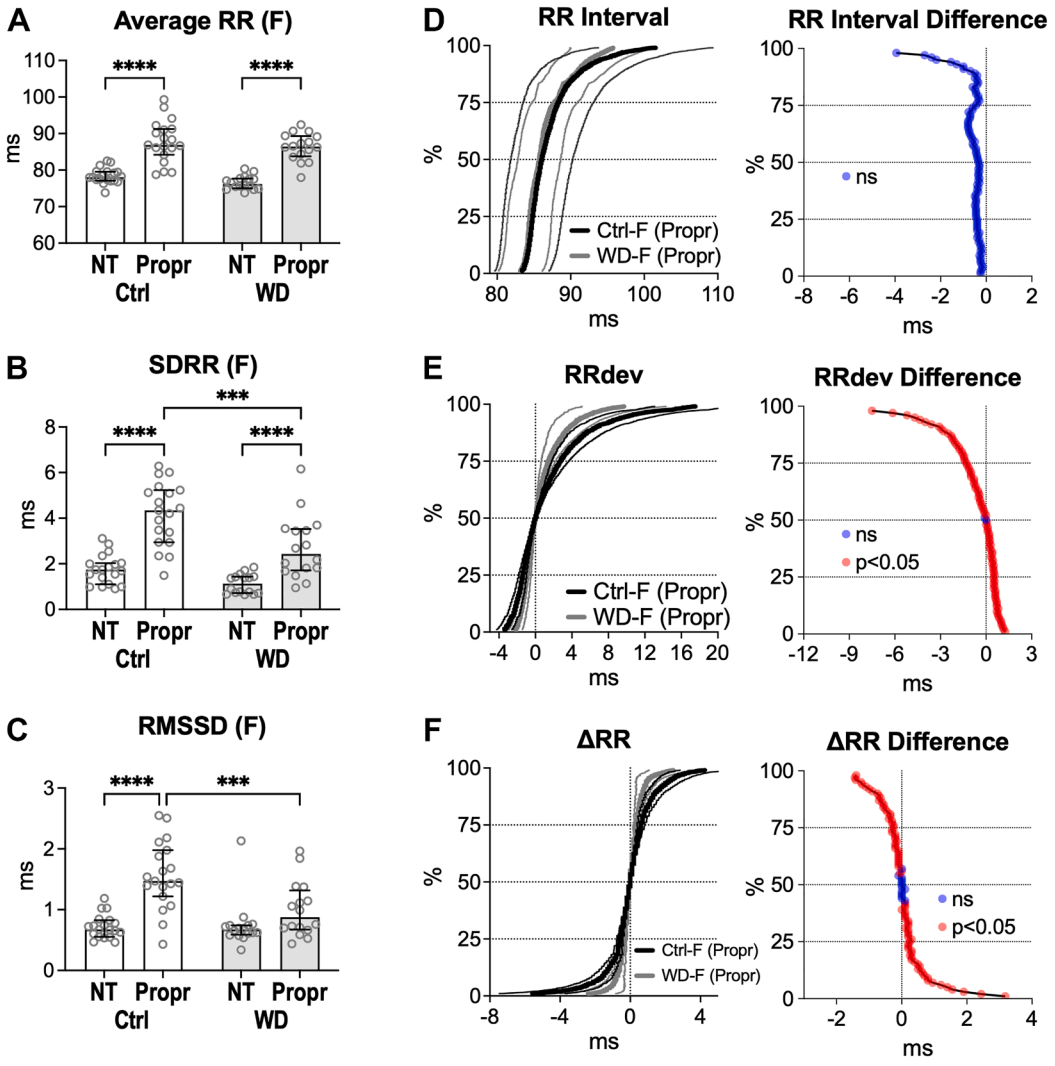

Figure 4 Effects of attenuation of sympathetic tone on R-R interval properties in female mice without and with metabolic syndrome. Quantitative data for R-R interval properties for Ctrl female mice (n = 19) and WD female mice (n = 16) in the absence (not treated [NT]) and presence of inhibition of sympathetic inputs by the β-adrenergic receptor (β-AR) blocker propranolol (Propr, 1 mg/kg body weight, intraperitoneally). **A–C:** Quantitative data for classical metrics of heart rate variability for Ctrl and WD mice in the absence and presence of β-AR blockade with Propr. Data are presented as medians and IQRs with dot plots. ***$P < .001$, and ****$P < .0001$ using a 2-way analysis of variance. **D–F:** Aggregate data for sortRR (panel D), sortRRdev (panel E), and sortΔRR (panel F) sequences for Ctrl (*black lines*) and WD (*gray lines*) mice after treatment with Prop are presented as median ± MAD. Right panels illustrate shift functions reporting differences in R-R interval duration, RRdev, and ΔRR between WD and Ctrl mice at each exact percentile level. For shift functions, significant adjusted *P* values (<.05) are shown with *red dots* whereas ns differences are shown with *blue dots*. Abbreviations as in Figures 1–3.

Collectively, the analysis of the distribution of R-R interval properties reveals that MetS reduces the span of R-R interval duration and variation, indicating that MetS limits heart rhythm adjustments and prevents the lowering of heart rate.

MetS and contribution of sympathetic inputs–β-AR signaling to alterations in heart rate dynamics

To establish the role of the sympathetic branch of the autonomic nervous system in alterations in heart rate dynamics in mice with MetS, ECGs were collected from Ctrl and WD animals without treatment and after the acute administration of the β-AR blocker propranolol.[22,26]

In female animals, compared with the nontreated state, β-AR blockade increased average R-R interval duration and SDRR in both Ctrl and WD mice but RMSSD was significantly increased only in Ctrl mice (Figure 4A–4C). Thus, in the presence of the β-AR blocker, average R-R interval duration was similar in the 2 groups of female animals, but SDRR and RMSSD were, respectively, 44% and 40% smaller in WD mice than in Ctrl animals.

Using distribution profiles, in the presence of β-AR blockade, sortRR sequences for Ctrl and WD female mice were comparable (Figure 4D). In contrast, RRdev and ΔRR had smaller absolute values in WD mice, compared with corresponding percentiles in Ctrl animals (Figure 4E and 4F). Similar findings were observed in male animals (Supplemental Figure 4).

When comparing male and female animals in the presence of sympathetic tone inhibition, no differences were observed for Ctrl animals whereas for WD male mice

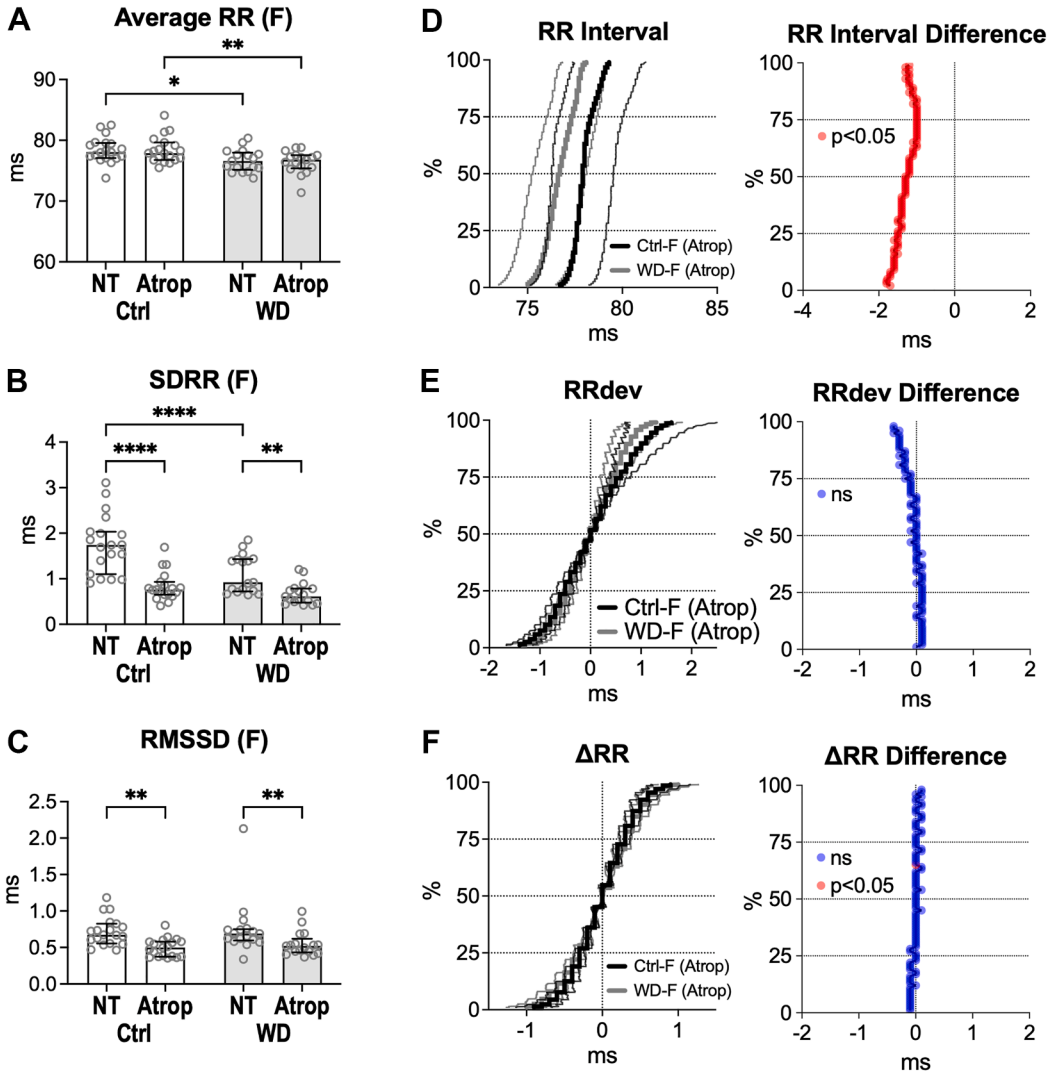

Figure 5 Effects of attenuation of parasympathetic tone on R-R interval properties in female mice without and with metabolic syndrome. Quantitative data for R-R interval properties for Ctrl female mice (n = 19) and WD female mice (n = 17) in the absence (NT) and presence of inhibition of parasympathetic inputs by the muscarinic receptor antagonist atropine (Atrop, 0.5 mg/kg body weight, intraperitoneally). **A–C:** Quantitative data for classical metrics of heart rate variability for Ctrl and WD mice in the absence and presence of Atrop. Data are presented as medians and IQRs with dot plots. *$P < .05$, **$P < .01$, and ****$P < .0001$ using a 2-way analysis of variance. **D–F:** Aggregate data for sortRR (panel D), sortRRdev (panel E), and sortΔRR (panel F) sequences for Ctrl (*black lines*) and WD (*gray lines*) mice after treatment with Atrop are presented as median ± MAD. Right panels illustrate shift functions reporting differences in R-R interval duration, RRdev, and ΔRR between WD and Ctrl mice at each exact percentile. For shift functions, significant adjusted *P* values (<.05) are shown with *red dots* whereas ns differences are shown with *blue dots*. Abbreviations as in Figures 1–4.

SDRR was attenuated compared with female WD animals (Supplemental Figure 5A–5C). However, when using distribution profiles, in the presence of β-AR blockade, R-R interval properties for Ctrl and WD mice were similar in female and male animals (Supplemental Figure 5D–5F).

Thus, inhibition of the sympathetic–β-AR axis increases the R-R interval duration and its variability in Ctrl and WD mice, leading to comparable R-R interval duration and R-R interval span for the 2 groups of animals. However, attenuation of sympathetic tone intensified the tendency of MetS to reduce short- and long-term R-R interval variability.

MetS and contribution of the parasympathetic tone to alterations in heart rate dynamics

The findings that the β-AR blockade strengthened differences in R-R interval variability between Ctrl and WD mice supported the possibility that factors other than β-AR signaling are altered by the obesogenic diet. Thus, to address the role of the parasympathetic tone in the consequences of the Western diet on heart rhythm dynamics, ECGs were collected from Ctrl and WD animals without treatment and after the acute administration of atropine, which antagonizes the activity of the parasympathetic neurotransmitter acetylcholine.[22,26]

Using classical HRV metrics, atropine had no effect on the average R-R interval duration in both Ctrl and WD

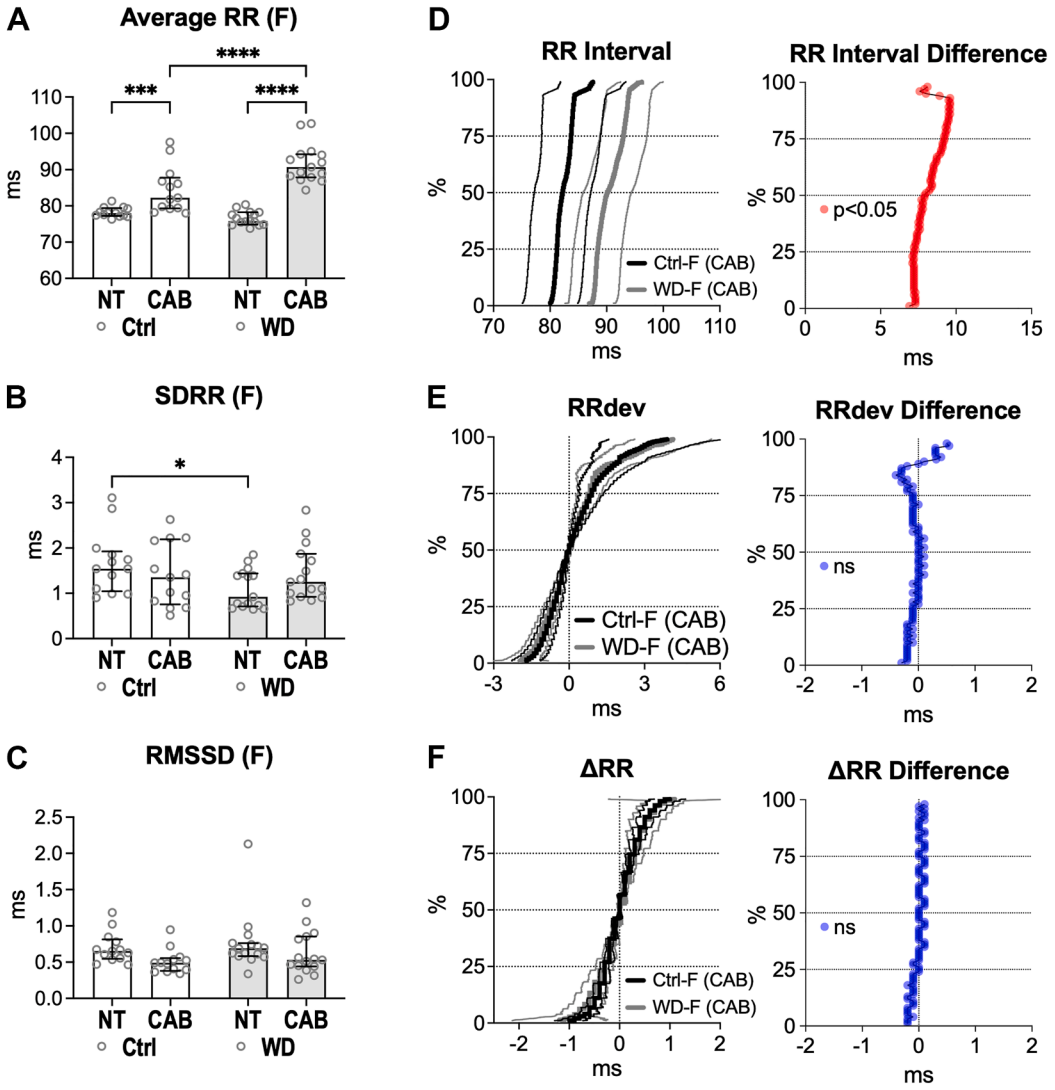

Figure 6 Effects of combined attenuation of sympathetic and parasympathetic tone on R-R interval properties in female mice without and with metabolic syndrome. Quantitative data for R-R interval properties for Ctrl female mice (n = 13) and WD female mice (n = 15) in the absence (NT) and presence of inhibition of sympathetic and parasympathetic inputs by combined administration of atropine (0.5 mg/kg body weight, intraperitoneally [i.p.]) and propranolol (1 mg/kg body weight, i.p.) to achieve combined autonomic block (CAB). **A–C:** Quantitative data for classical metrics of heart rate variability for Ctrl and WD mice in the absence and presence of CAB. Data are presented as medians and IQRs with dot plots. *$P < .05$, ***$P < .001$, and ****$P < .0001$ using a 2-way analysis of variance. **D–F:** Aggregate data for sortRR (panel D), sortRRdev (panel E), and sortΔRR (panel F) sequences for Ctrl (*black lines*) and WD (*gray lines*) mice after treatment with CAB are presented as median ± MAD. Right panels illustrate shift functions reporting differences in R-R interval duration, RRdev, and ΔRR between WD and Ctrl mice at each exact percentile. For shift functions, significant adjusted *P* values (<.05) are shown with *red dots* whereas ns differences are shown with *blue dots*. Abbreviations as in Figures 1–4.

female mice. However, compared with the nontreated state, atropine reduced SDRR and RMSSD in both Ctrl and WD female mice (Figure 5A–5C). Hence, in the presence of the parasympathetic antagonist atropine, the average R-R interval duration remained shorter in WD female mice than in Ctrl animals. Still, SDRR and RMSSD were comparable for the 2 groups of mice.

Using distribution profiles, in the presence of atropine, R-R intervals were shorter in WD female mice than in Ctrl female animals (Figure 5D) whereas RRdev and ΔRR were similar between the 2 groups of female mice (Figure 5E and 5F).

Effects of atropine in Ctrl and WD female mice were also observed in male animals, but this intervention was less effective in abrogating differences in SDRR, RMSSD, sortRRdev, and sortΔRR between WD and Ctrl male mice (Supplemental Figure 6). As a result, when comparing male and female animals in the presence of parasympathetic tone inhibition, indices of R-R interval variability were larger in male mice, than in female animals, for the Ctrl and, in part, WD groups (Supplemental Figure 7).

Thus, inhibition of parasympathetic inputs has minor effects on the R-R interval duration in Ctrl and WD mice but it reduces R-R interval variability, attenuating differences between the 2 groups of mice. The consequences of parasympathetic inhibition in the setting of MetS appear to be attenuated in male animals.

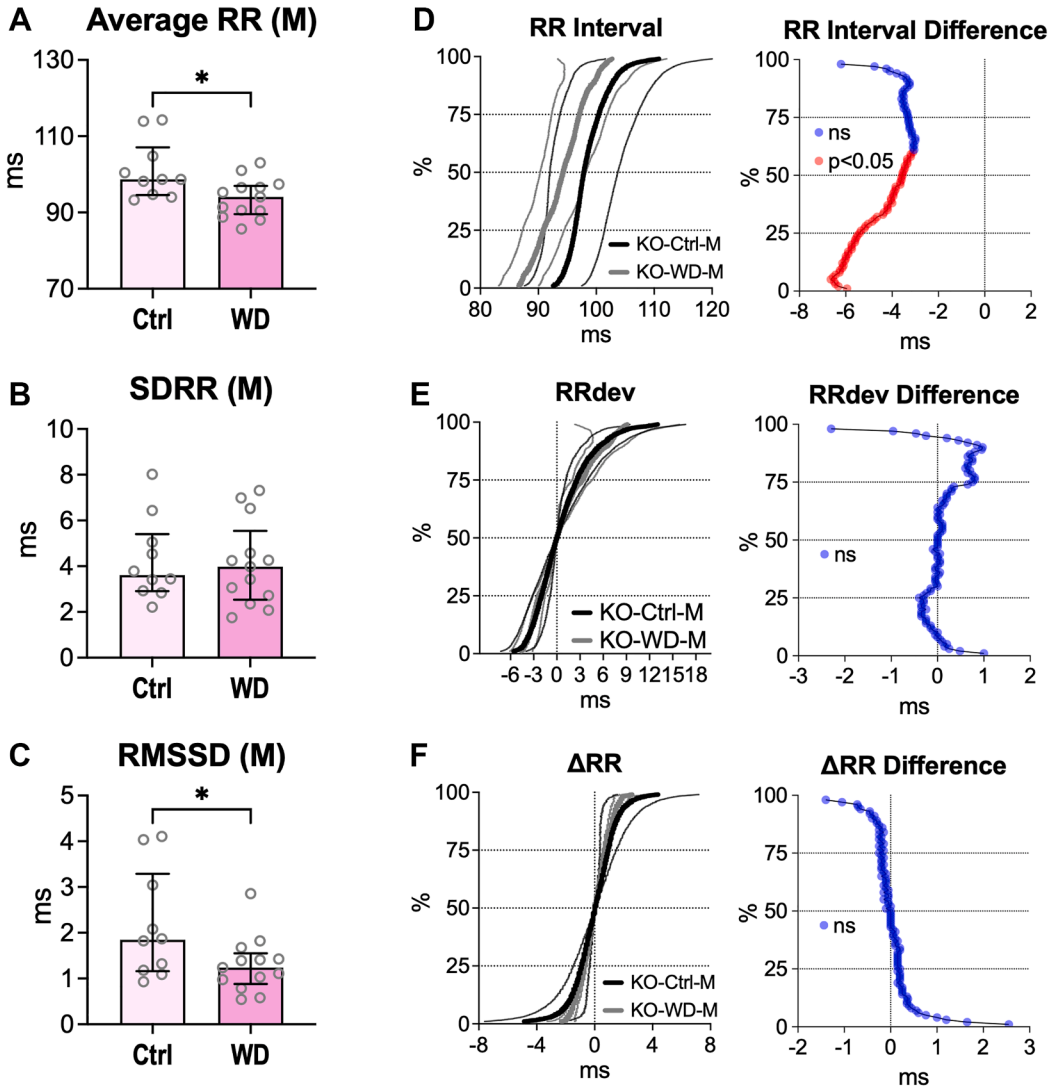

Figure 7 Effects of the Western diet on heart rhythm dynamics in male mice lacking β-ARs. Quantitative data for heart rate variability (HRV) parameters for Ctrl male β-AR global knockout mice (BAR-KO mice) (*light pink bars*, n = 10) and WD male BAR-KO mice (*dark pink bars*, n = 13) for ∼4 months on the respective diets. **A–C:** Quantitative data for classical metrics of HRV for Ctrl and WD BAR-KO mice are presented as medians and IQRs with dot plots. *$P <$ .05 using an unpaired *t* test or a Mann-Whitney *U* test. **D–F:** Aggregate data for sortRR (panel D), sortRRdev (panel E), and sortΔRR (panel F) sequences and related shift functions for Ctrl BAR-KO mice (KO-Ctrl-M, *black lines*) and WD BAR-KO mice (KO-WD-M, *gray lines*) are presented as median ± MAD (left panel). Right panels illustrate shift functions reporting differences in R-R interval duration, RRdev, and ΔRR between WD and Ctrl BAR-KO mice at each exact percentile. For shift functions, significant adjusted *P* values (<.05) are shown with *red dots* whereas ns differences are shown with *blue dots*. Abbreviations as in Figures 1–4.

MetS and combined contribution of the sympathetic and parasympathetic tone to alterations in heart rate dynamics

To test the possibility that combined alterations in sympathetic and parasympathetic inputs account for alterations in heart rate properties induced by the Western diet, ECGs were obtained in mice after the acute and simultaneous administration of atropine and propranolol to achieve CAB.

Using classical HRV metrics, in Ctrl and WD female mice, CAB increased the average R-R interval duration by 5% and 20%, respectively, but had no significant effects on SDRR and RMSSD, in comparison to the nontreated state. Therefore, in the presence of CAB, the average R-R interval duration was 10% longer in WD female mice, than in Ctrl mice, whereas SDRR and RMSSD were comparable in the 2 groups of female animals (Figure 6A–6C).

Using distribution profiles, in the presence of CAB, the R-R interval duration was longer in WD female mice than in Ctrl female animals (Figure 6D). In contrast, RRdev and ΔRR were comparable in the 2 groups of female mice (Figure 6E and 6F). Generally, alterations induced by CAB in female mice were also observed in male animals (Supplemental Figure 8), and no major differences were observed when comparing the 2 sexes for Ctrl and WD mice with CAB.

Collectively, the combined inhibition of the sympathetic and parasympathetic inputs of the autonomic nervous system

reverses differences in R-R interval durations between Ctrl and WD mice and normalizes their R-R interval variation, supporting the contribution of the 2 axes of the autonomic nervous system to the altered heart rhythm dynamics occurring with MetS.

MetS and heart rate dynamics in the absence of β-AR signaling

To clarify the contribution of the sympathetic and parasympathetic tone to alterations in HRV occurring with MetS, BAR-KO mice[27] were introduced. As previously reported,[49] BAR-KO mice had a reduced heart rate and HRV compared with mice with intact β-AR signaling (Supplemental Figure 9). These findings were confirmed by distribution profile analysis (Supplemental Figure 10). Thus, female and male BAR-KO mice were fed the Western diet or regular chow for ∼4 months, and ECGs were collected for the evaluation of R-R interval properties.

Interestingly, female BAR-KO mice on the regular or Western diet had comparable R-R interval duration and HRV parameters, using time-domain (Supplemental Figure 11A–11C), frequency-domain, and nonlinear analyses. Moreover, sortRR, sortRRdev, and sortΔRR sequences were similar for the 2 groups of female mice (Supplemental Figure 11D–11F). In contrast, for the male sex, R-R interval duration and RMSSD were reduced by 5% and 33%, respectively, in WD BAR-KO mice in comparison to Ctrl BAR-KO animals (Figure 7A–7C). Moreover, using distribution profiles, WD male BAR-KO mice had shorter R-R interval durations in correspondence with short R-R intervals whereas RRdev and ΔRR were comparable (Figure 7D–7F). When evaluating the 2 sexes, no significant differences were observed between female and male BAR-KO mice fed either regular chow or Western diet, using classical and sortRR analyses.

To clarify the contribution of parasympathetic inputs to heart rate dynamics in Ctrl and WD BAR-KO mice, ECGs were collected in the absence and presence of acute atropine treatment. For the 2 sexes, atropine attenuated indices of R-R interval variability in both Ctrl and WD BAR-KO mice (Supplemental Figure 12). After the treatment with atropine, parameters of HRV and sorted profiles were comparable between Ctrl and WD BAR-KO mice for the 2 sexes, and no differences between male and female animals were observed for the Ctrl and WD groups.

Since atropine abrogated differences in R-R interval properties between Ctrl and WD male BAR-KO mice, the possibility was raised that alterations in parasympathetic input are involved in the process. Thus, the functionality of parasympathetic activity in Ctrl and WD BAR-KO mice was tested by evoking the baroreceptor reflex by administration of phenylephrine, a potent vasoconstrictor.[33,34] For the 2 sexes, the hypertensive challenge lowered heart rate and enhanced HRV in both Ctrl and WD BAR-KO mice, consistent with baroreflex-mediated parasympathetic tone activation. Importantly, for female BAR-KO mice, HRV parameters in the presence of phenylephrine were comparable in Ctrl and WD animals (Supplemental Figure 13). In contrast, for male animals treated with phenylephrine, SDRR, RMSSD, total power, and the profile of ΔRR were reduced in WD male mice compared with Ctrl BAR-KO mice (Figure 8), revealing an attenuated activation of the parasympathetic–muscarinic receptor axis in male mice with MetS.

Collectively, loss of β-ARs increases the R-R interval duration and its variability and largely attenuates the consequences of MetS on R-R interval properties. These findings support the key role of the sympathetic–β-AR signaling axis in alterations in heart rate dynamics in metabolic disorders and reveal the contribution of parasympathetic withdrawal to attenuating R-R interval variation, particularly in male animals.

Validation of the custom algorithm

To evaluate the capability of the newly developed algorithm to detect alterations in heart rhythm dynamics and potential applicability to clinical data, validation tests were introduced.

With the newly developed analytical approach, compared with Ctrl animals, male and female WD mice presented an altered span, distribution, and variation of R-R intervals (see Figure 3). Similarly, time-domain, frequency-domain, and Poincaré plot–derived nonlinear parameters of HRV were altered in WD mice (see Figure 2 and Supplemental Figure 3). Thus, to further validate the correctness of the results obtained with the custom algorithm, a nonlinear method based on SampEn was introduced as a complexity measure of R-R intervals.[39] Interestingly, the SampEn approach identified significant differences between Ctrl and WD mice for the 2 sexes (Supplemental Figure 14).

Thus, the alignment of sortRR analysis findings with results from classical HRV metrics and SampEn supports the capability of the custom algorithm to detect alterations in heart rhythm properties.

Given the differences in waveform morphology and R-R interval duration between ECGs from rodents and human subjects, we evaluated the compatibility of the novel algorithm for clinical ECG analysis using a publicly available data set.[43–45] Visual inspection confirmed that the algorithm accurately detected R waves in human ECGs and correctly rejected ectopic beats and artifactual peaks (Supplemental Figure 15). Using a small cohort of data from male subjects at the age of 18–19 and 60–64 years, we observed qualitative differences in R-R interval span, distribution, and variation (Figure 9). Importantly, sortRR detected the age-related prolongation of the R-R interval whereas the narrower ranges of sortRR, sortRRdev, and sortΔRR in older subjects reflected the reduction in HRV previously reported to occur with aging.[44,50]

Thus, these initial tests support the applicability of the custom algorithm to ECGs from human subjects.

Discussion

The results of this study document that MetS, induced by Western diet feeding, alters heart rate dynamics in mice, a condition consistent with modifications of cardiac sympathovagal balance. Using classical metrics of HRV, both male and female mice fed the Western diet had reduced long-term R-R

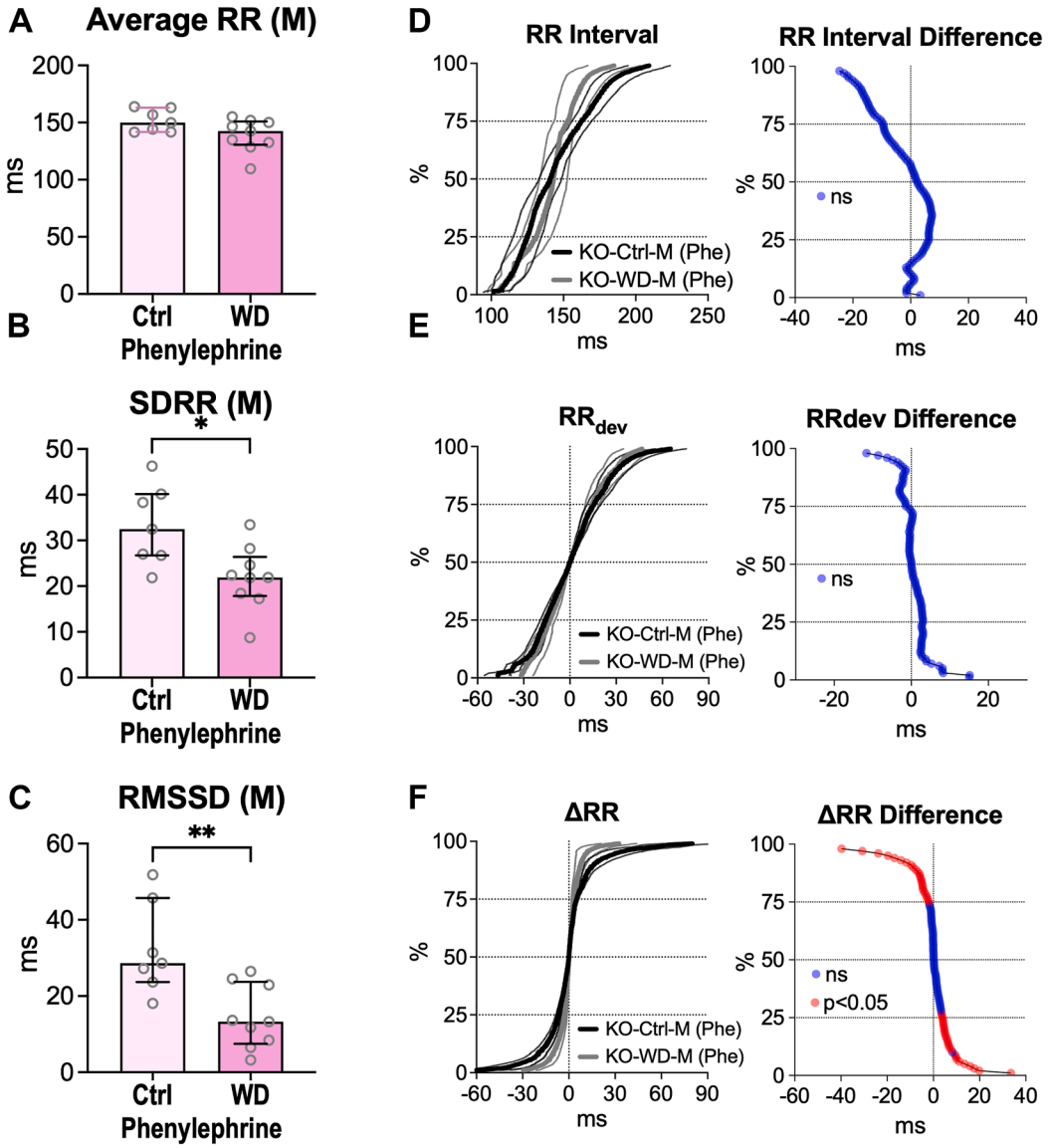

Figure 8 Baroreflex activation in BAR-KO male mice without and with metabolic syndrome. Quantitative data for R-R interval properties for Ctrl (*light pink bars*, n = 7) and WD (*dark pink bars*, n = 9) male BAR-KO mice in response to phenylephrine-induced hypertension (phenylephrine, 3 mg/kg body weight, intraperitoneally). For this protocol, ECGs were collected over a period of 20 minutes. **A–C:** Data are presented as medians and IQRs with dot plots. $*P < .05$ and $**P < .01$ using an unpaired *t* test or a Mann-Whitney *U* test. **D–F:** Aggregate data for sortRR (panel D), sortRRdev (panel E), and sortΔRR (panel F) sequences and related shift functions for Ctrl (*black lines*) and WD (*gray lines*) male BAR-KO mice after treatment with phenylephrine are presented as median ± MAD (left panel). Right panels illustrate shift functions reporting differences in R-R interval duration, RRdev, and ΔRR between WD and Ctrl BAR-KO mice at each exact percentile. For shift functions, significant adjusted *P* values (<.05) are shown with *red dots* whereas ns differences are shown with *blue dots*. Abbreviations as in Figures 1–4 and 7.

interval variability and, in the presence of sympathetic inhibition, both long-term variability and short-term variability were reduced, indicating that sympathoexcitation and parasympathetic tone withdrawal occur with MetS.

To complement the results obtained with standard analysis of HRV, a custom analytical approach was introduced to examine the consequences of MetS on distribution, functional range, and variation of R-R intervals. This approach revealed that R-R intervals of brief duration were comparable in Ctrl and WD mice whereas long R-R intervals were significantly shorter in animals with MetS. Moreover, R-R interval span was substantially reduced in mice on the Western diet. These findings support the notion that MetS constrains the functional range of heart rate and interferes with the ability of the heart to adapt to low beating rates. Although the response of heart rate to exercise and recovery was not directly assessed in this study, the observed patterns are reminiscent of the chronotropic incompetence and impaired heart rate recovery, both commonly reported in patients with MetS.[51–54] Notably, a diminished heart rate response to physical exertion, along with a delayed return to resting level postexercise, is a significant predictor of both coronary heart disease and increased mortality risk.[55,56] Thus, measurements of the span of R-R interval durations and the distribution of R-R interval

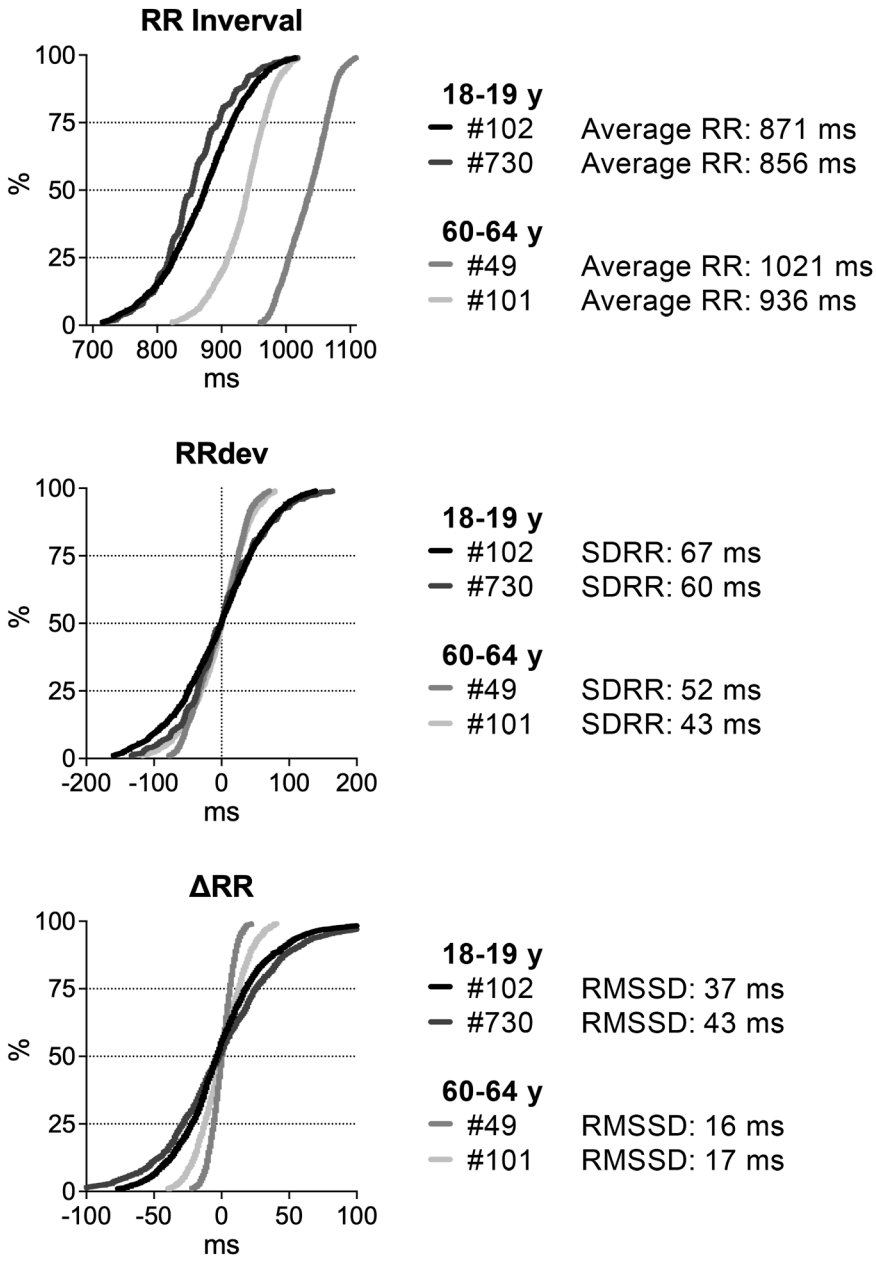

Figure 9 sortRR analysis of ECGs from human subjects detects alterations in the span, distribution, and variation of R-R interval durations with aging. **A–C:** sortRR (panel A), sortRRdev (panel B), and sortΔRR (panel C) sequences for male human subjects at the age of 18–19 and 60–64 years obtained from publicly available ECG recordings from the PhysioNet database (see text). Average R-R interval duration, SDRR, and RMSSD for each subject are reported. Abbreviations as in Figures 1–3.

variations offer important insights into the chronotropic competence of the heart and associated cardiovascular risks.

The observation that with MetS the heart does not function at lower heart rates has significant implications for cardiovascular abnormalities linked to the condition. Elevated heart rates may worsen diastolic dysfunction by shortening LV filling time and reducing stroke volume, factors that could contribute to the symptomatology of HFpEF. Surprisingly, studies investigating heart rate–lowering therapies in patients with HFpEF have yielded mixed results,[57] thereby weakening the proposed causal link between elevated heart rate and disease progression. Nevertheless, the possibility remains that the efficacy of heart rate–lowering interventions depends on the severity of the disease and/or that the beneficial effects are confined to specific heart rate ranges, allowing optimal LV filling. In this regard, with the increasing precision of wearable technologies,[58] it is now feasible to implement monitoring of heart rate in conjunction with other health metrics to gain information on the relationship between heart rate and symptom manifestation in patients with HFpEF. Importantly, initial tests using publicly available ECG recordings[43–45] have validated the capability of our analytical approach to evaluate distribution, functional range, and variation of R-R intervals in human subjects

and to detect alterations in HRV occurring with aging.[44,50] Thus, our custom algorithm may provide a solid platform to identify R-R interval ranges associated with symptom relief, offering valuable insight for the assessment of the effects of heart rate–lowering interventions.

In this study, pharmacological approaches were used to determine the contribution of the sympathetic and parasympathetic branches of the autonomic nervous system to alterations in heart rhythm dynamics occurring with MetS. The acute inhibition of the sympathetic–β-AR axis abrogated differences in average R-R interval duration and normalized the profile of sortRR sequences for the 2 groups of animals, suggesting that sympathoexcitation accounts for the shorter R-R intervals observed with MetS. However, in the presence of β-AR blockade, R-R interval variability was reduced in mice with MetS, indicating that factors other than sympathoexcitation contribute to the process. In this regard, inhibition of the parasympathetic–muscarinic receptor axis suppressed differences in R-R interval variability between WD and Ctrl animals, corroborating the role of parasympathetic withdrawal in the reduced HRV occurring with MetS. Interestingly, the combined inhibition of the sympathetic and parasympathetic axes eliminated and/or reversed differences in R-R interval properties between the 2 groups of mice, substantiating the involvement of the 2 branches of the autonomic nervous system in the modifications of heart rate dynamics occurring with MetS.

Pharmacological modulation of the autonomic nervous system is rarely used to evaluate HRV in clinical research.[59–61] However, autonomic blockade has served to assess intrinsic sinus node function, as in the case of patients with suspected inappropriate sinus tachycardia[62] or sick sinus syndrome.[63] Despite the limited dependence of clinical studies on pharmacological interventions, researchers have more commonly relied on physical maneuvers, including exercise and head-up tilt testing, in conjunction with HRV analysis, to evaluate autonomic nervous system responsiveness.[64,65] Importantly, the capability of the custom algorithm to compute R-R interval span and distribution makes it well-suited for studies aimed at tracking alterations in heart rate induced by physical maneuvers. This competence underscores the translational potential of the algorithm for clinical research and diagnostic applications.

The introduction of mice lacking β-AR in our analysis has allowed us to clarify the contribution of the 2 limbs of the autonomic nervous system to heart rhythm dynamics in Ctrl and WD mice. Moreover, BAR-KO mice have provided the opportunity to validate results obtained with the custom analytical approach by using an independent rodent model previously reported to present reduced HRV.[49] The chronic loss of β-AR in BAR-KO mice attenuated the effects of Western diet feeding on heart rhythm dynamics. HRV parameters were comparable in Ctrl and WD female BAR-KO mice, but male BAR-KO mice with MetS presented shortened R-R interval duration and attenuated short-term variability. These differences were abolished by atropine, substantiating the contribution of parasympathetic tone withdrawal to mediate the behavior of male animals with MetS. This possibility was corroborated by the finding that baroreflex response induced by phenylephrine challenge was impaired in male BAR-KO animals with MetS, but not in female mice.

As previously discussed, the acute inhibition of β-AR in C57Bl/6 mice amplified differences in short- and long-term R-R interval variability between Ctrl and WD animals, revealing withdrawal of parasympathetic tone with MetS. In contrast, chronic deletion of β-AR in BAR-KO mice eliminated differences in long-term variability between Ctrl and WD animals, supporting the possibility that defects of parasympathetic tone with MetS are attenuated in BAR-KO mice. These findings raise the possibility that the loss of β-AR may confer cardioprotective properties by preventing the effects of sympathoexcitation on the manifestations and development of MetS.[66] This possibility, however, requires further investigation.

The detection of sympathoexcitation and parasympathetic tone withdrawal in mice with MetS via R-R interval analysis aligns with the findings of elevated myocardial catecholamines in WD mice, along with increased cyclic adenosine monophosphate levels and protein kinase A activity in myocytes.[26] Altered sympathovagal balance at the sinoatrial node manifests changes in heart rate dynamics and reduced R-R interval span, whereas ventricular myocytes exhibit potentiated electromechanical coupling and increased contractility. These functional adaptations, mediated by the sympathetic–β-AR signaling axis, appear to compensate for the increased cardiac workload associated with MetS, possibly because of reduced vascular compliance and increased circulating blood volume.[67,68] Interestingly, acute β-AR blockade unmasked cardiac defects in WD mice fed the Western diet,[26] underscoring the key homeostatic role of autonomic regulation in MetS. However, whether the chronotropic and inotropic effects of sympathoexcitation are accompanied by maladaptive consequences remains unclear. Similar considerations apply to downstream targets of the α-AR–phospholipase C axis and noncanonical β-AR signaling pathways,[69,70] which appear chronically activated in MetS. Therefore, tracking the R-R interval profile could provide important insights into autonomic function and its downstream consequences during disease progression.

Features observed in Ctrl and WD male and female mice with intact or deleted β-AR signaling indicate that heart rate dynamics with MetS manifests subtle sexual dimorphisms. In fact, while increased sympathetic tone and reduced parasympathetic input are shared by the 2 sexes, parasympathetic withdrawal is more pronounced in male animals. Interestingly, a study involving the deprivation of sex hormones in rats fed a high-fat diet found that the relatively preserved cardiac autonomic function observed in female rats, compared with male rats, was secondary to the protective effects of estrogen.[71] This mechanism may also underlie the sex-specific differences observed in our experimental groups. These results are, however, at variance with studies in humans reporting that women with MetS show clear signs of reduced HRV, assessed by the SDRR duration, whereas in men this trend was not significant. Nevertheless, reduced LF oscillations

with MetS were observed only in men.[72] Stronger systemic reaction to inflammation in women and a higher prevalence of central obesity in men have been proposed as contributing factors to sex-related disparities in HRV.[72] However, the underlying causes of sexual dimorphism in relation to cardiac autonomic balance in the settings of metabolic disorders, in both humans and experimental animals, warrant further comparative investigation.

Longitudinal studies in humans have documented a strong association between altered HRV, metabolic abnormalities, and the incidence of cardiovascular problems.[6,8] These investigations substantiate the predictive value of HRV assessments for the manifestation of MetS and raise the possibility of a causative relation between altered sympathovagal balance and the development of cardiometabolic disease. Importantly, recent systematic reviews and meta-analyses have reported that patients with MetS have reduced time-domain and frequency-domain parameters of HRV,[72–74] which is consistent with cardiac autonomic dysregulation in metabolic disorders. Specifically, a meta-analysis of 19 studies revealed that, when combining data from men and women, the time-domain parameters SDRR and RMSSD and the frequency-domain parameters HF and LF were reduced in individuals with MetS compared with control subjects.[72] Interestingly, using classical HRV analysis, our observations in rodents align with the results obtained from patients with MetS. In fact, as reported for human subjects, we found that mice on the Western diet have reduced SDRR and attenuation of power associated with the R-R interval oscillations, using frequency-domain analysis. Also, RMSSD was reduced in mice with MetS, although this trend did not reach statistical significance in the cohort of female animals. Notably, reduction in the neural baroreflex pathway has been reported for patients with metabolic disorders[75] and this feature, which is indicative of autonomic dysfunction, has also been uncovered in male mice with MetS using phenylephrine challenge. Although the reported reduction in SDRR in patients with MetS is presumptive of a narrow R-R interval span, further investigations are needed to evaluate whether the functional range of the R-R interval and its distribution profile are affected in individuals with metabolic disorders.

The average R-R interval duration and its standard deviation (SDRR) provide information on the mean behavior of the cardiac autonomic system for experimental subjects over the period of examination. However, these parameters cannot accurately report the ranges of variation and distribution of R-R interval durations throughout the acquisition period, limiting the information that can be extracted from the collected data. To overcome this constraint, the sorting of R-R interval durations over percentile ranks was introduced to assess the distribution of R-R intervals and to identify minimal and maximal R-R interval durations, which are key indicators of the activity of the autonomic nervous system for experimental subjects. Using this approach, the analysis of the distribution profile not only confirmed the result of standard analysis that the average R-R interval duration is reduced in female animals with MetS but also reported that maximal heart rates are comparable in the 2 groups of mice whereas lower heart rates are substantially elevated in female animals with MetS. An attenuated form of this behavior was also present in male animals, but the classical linear analysis did not capture this feature. Thus, the distribution analysis of R-R interval properties provides important quantitative and qualitative assessments of HRV, complementing standard metrics for the evaluation of heart rhythm dynamics.

Several analytical approaches have been introduced to enhance the precision of HRV parameters to examine the contribution of the 2 branches of the autonomic nervous system, as well as other circulating and systemic factors, to the regulation of heart rate. Thus, traditional time-domain and frequency-domain indices[23] have been complemented with nonlinear metrics based on fractals and chaos theory[20,76] and, more recently, with machine learning models.[77] In the setting of metabolic disorders, clinical studies have documented that nonlinear measures of HRV have the capability to detect diabetes accurately[78] and to link the reduction in SampEn with progressive autonomic dysfunction in patients with MetS.[79] Similarly, another study has validated the utility of machine learning models to predict diabetes using HRV.[80] The analytical approach developed in the present study offers the unique capability to define R-R interval ranges that may be influenced by health status and therapeutic interventions. This novel feature underscores the potential of this investigative tool for basic cardiovascular studies and clinical screening.

Acknowledgments

We thank Andrea Filardo, Alessandra Franco, Trisha Mukherjee, and Robin Ni at New York Medical College for their technical assistance.

Funding Sources: This work was supported by the American Heart Association (24TPA1303897, to Dr Rota; 24CDA1269532, to Dr Bisserier), the National Institutes of Health/National Heart, Lung, and Blood Institute (K01HL159038-01A1 and R25HL146166, to Dr Bisserier), the American Thoracic Society Research Program (23-24U1, to Dr Bisserier), and intramural resources at New York Medical College (NYMC), including funds from the SOM/WMC TSI Funding Grant Program awarded from the NYMC School of Medicine of the Touro College and University System and Touro Seed and Bridge Funding Grant Program awards from the Biomedical and Health Sciences Research Council of Touro University. Ms Volney was supported by a fellowship from the School of Medicine at NYMC.

Disclosures: The authors have no conflicts of interest to disclose.

Authorship: All authors attest they meet the current ICMJE criteria for authorship.

Ethics Statement: The research reported in this article adhered to Animal Research: Reporting of In Vivo Experiments guidelines and the *Guide for the Care and Use of Laboratory Animals*. Animal housing and experiments were approved by the local animal care committees (Institutional Animal Care and Use Committee) of New York Medical College.

Appendix

Supplementary data

Supplementary data associated with this article can be found in the online version at https://doi.org/10.1016/j.hroo.2025.11.025.

References

1. Martin SS, Aday AW, Allen NB, et al. 2025 Heart disease and stroke statistics: a report of US and Global data from the American Heart Association. Circulation 2025;151:e41–e660.
2. Alberti KG, Eckel RH, Grundy SM, et al. Harmonizing the metabolic syndrome: a joint interim statement of the International Diabetes Federation Task Force on Epidemiology and Prevention; National Heart, Lung, and Blood Institute; American Heart Association; World Heart Federation; International Atherosclerosis Society; and International Association for the Study of Obesity. Circulation 2009;120:1640–1645.
3. Ayalon N, Gopal DM, Mooney DM, et al. Preclinical left ventricular diastolic dysfunction in metabolic syndrome. Am J Cardiol 2014;114:838–842.
4. de las Fuentes L, Brown AL, Mathews SJ, et al. Metabolic syndrome is associated with abnormal left ventricular diastolic function independent of left ventricular mass. Eur Heart J 2007;28:553–559.
5. Azevedo A, Bettencourt P, Almeida PB, et al. Increasing number of components of the metabolic syndrome and cardiac structural and functional abnormalities—cross-sectional study of the general population. BMC Cardiovasc Disord 2007;7:17.
6. Wulsin LR, Horn PS, Perry JL, Massaro JM, D'Agostino RB. Autonomic imbalance as a predictor of metabolic risks, cardiovascular disease, diabetes, and mortality. J Clin Endocrinol Metab 2015;100:2443–2448.
7. Wulsin LR, Horn PS, Perry JL, Massaro JM, D'Agostino RB Sr. The contribution of autonomic imbalance to the development of metabolic syndrome. Psychosom Med 2016;78:474–480.
8. Licht CM, de Geus EJ, Penninx BW. Dysregulation of the autonomic nervous system predicts the development of the metabolic syndrome. J Clin Endocrinol Metab 2013;98:2484–2493.
9. Huggett RJ, Scott EM, Gilbey SG, Stoker JB, Mackintosh AF, Mary DA. Impact of type 2 diabetes mellitus on sympathetic neural mechanisms in hypertension. Circulation 2003;108:3097–3101.
10. Huggett RJ, Burns J, Mackintosh AF, Mary DA. Sympathetic neural activation in nondiabetic metabolic syndrome and its further augmentation by hypertension. Hypertension 2004;44:847–852.
11. Azulay N, Olsen RB, Nielsen CS, et al. Reduced heart rate variability is related to the number of metabolic syndrome components and manifest diabetes in the sixth Tromsø study 2007–2008. Sci Rep 2022;12:11998.
12. Brubaker PH, Kitzman DW. Chronotropic incompetence: causes, consequences, and management. Circulation 2011;123:1010–1020.
13. Fukuda K, Kanazawa H, Aizawa Y, Ardell JL, Shivkumar K. Cardiac innervation and sudden cardiac death. Circ Res 2015;116:2005–2019.
14. Shen MJ, Zipes DP. Role of the autonomic nervous system in modulating cardiac arrhythmias. Circ Res 2014;114:1004–1021.
15. Shah SA, Kambur T, Chan C, Herrington DM, Liu K, Shah SJ. Relation of short-term heart rate variability to incident heart failure (from the Multi-Ethnic Study of Atherosclerosis). Am J Cardiol 2013;112:533–540.
16. Hanna P, Dacey MJ, Brennan J, et al. Innervation and neuronal control of the mammalian sinoatrial node a comprehensive atlas. Circ Res 2021;128:1279–1296.
17. Vassalle M, Catanzaro JN, Nett MP, Rota M. Essential role of diastolic oscillatory potentials in adrenergic control of guinea pig sino-atrial node discharge. J Biomed Sci 2009;16:101.
18. Vassalle M, Nett MP, Catanzaro JN, Rota M. Novel oscillatory mechanisms in the cholinergic control of guinea pig sino-atrial node discharge. J Cardiovasc Electrophysiol 2011;22:71–80.
19. MacDonald EA, Rose RA, Quinn TA. Neurohumoral control of sinoatrial node activity and heart rate: insight from experimental models and findings from humans. Front Physiol 2020;11:170.
20. Nicolini P, Ciulla MM, De Asmundis C, Magrini F, Brugada P. The prognostic value of heart rate variability in the elderly, changing the perspective: from sympathovagal balance to chaos theory. Pacing Clin Electrophysiol 2012;35:622–638.
21. Pizzo E, Berrettoni S, Kaul R, et al. Heart rate variability reveals altered autonomic regulation in response to myocardial infarction in experimental animals. Front Cardiovasc Med 2022;9:843144.
22. Comelli M, Meo M, Cervantes DO, et al. Rhythm dynamics of the aging heart: an experimental study using conscious, restrained mice. Am J Physiol Heart Circ Physiol 2020;319:H893–H905.
23. Shaffer F, Ginsberg JP. An overview of heart rate variability metrics and norms. Front Public Health 2017;5:258.
24. Nguyen S, Shao D, Tomasi LC, et al. The effects of fatty acid composition on cardiac hypertrophy and function in mouse models of diet-induced obesity. J Nutr Biochem 2017;46:137–142.
25. Mendes-Junior LG, Freitas-Lima LC, Oliveira JR, et al. The usefulness of short-term high-fat/high salt diet as a model of metabolic syndrome in mice. Life Sci 2018;209:341–348.
26. Pizzo E, Cervantes DO, Ripa V, et al. The cAMP/PKA signaling pathway conditions cardiac performance in experimental animals with metabolic syndrome. J Mol Cell Cardiol 2024;196:35–51.
27. Rohrer DK, Chruscinski A, Schauble EH, Bernstein D, Kobilka BK. Cardiovascular and metabolic alterations in mice lacking both β_1- and β_2-adrenergic receptors. J Biol Chem 1999;274:16701–16708.
28. Cervantes DO, Pizzo E, Ketkar H, et al. Scn1b expression in the adult mouse heart modulates Na^+ influx in myocytes and reveals a mechanistic link between Na^+ entry and diastolic function. Am J Physiol Heart Circ Physiol 2022;322:H975–H993.
29. Pizzo E, Cervantes DO, Ketkar H, et al. Phosphorylation of cardiac sodium channel at Ser571 anticipates manifestations of the aging myopathy. Am J Physiol Heart Circ Physiol 2024;326:H1424–H1445.
30. Sorrentino A, Borghetti G, Zhou Y, et al. Hyperglycemia induces defective Ca^{2+} homeostasis in cardiomyocytes. Am J Physiol Heart Circ Physiol 2017;312:H150–H161.
31. Signore S, Sorrentino A, Borghetti G, et al. Late Na^+ current and protracted electrical recovery are critical determinants of the aging myopathy. Nat Commun 2015;6:8803.
32. Meo M, Meste O, Signore S, et al. Reduction in Kv current enhances the temporal dispersion of the action potential in diabetic myocytes: insights from a novel repolarization algorithm. J Am Heart Assoc 2016;5:e003078.
33. Gehrmann J, Hammer PE, Maguire CT, Wakimoto H, Triedman JK, Berul CI. Phenotypic screening for heart rate variability in the mouse. Am J Physiol Heart Circ Physiol 2000;279:H733–H740.
34. Uechi M, Asai K, Osaka M, et al. Depressed heart rate variability and arterial baroreflex in conscious transgenic mice with overexpression of cardiac Gsα. Circ Res 1998;82:416–423.
35. D'Souza A, Bucchi A, Johnsen AB, et al. Exercise training reduces resting heart rate via downregulation of the funny channel HCN4. Nat Commun 2014;5:3775.
36. Leoni AL, Marionneau C, Demolombe S, et al. Chronic heart rate reduction remodels ion channel transcripts in the mouse sinoatrial node but not in the ventricle. Physiol Genomics 2005;24:4–12.
37. Moen JM, Matt MG, Ramirez C, et al. Overexpression of a neuronal type adenylyl cyclase (type 8) in sinoatrial node markedly impacts heart rate and rhythm. Front Neurosci 2019;13:615.
38. Roy B, Ghatak S. Nonlinear methods to assess changes in heart rate variability in type 2 diabetic patients. Arq Bras Cardiol 2013;101:317–327.
39. Richman JS, Moorman JR. Physiological time-series analysis using approximate entropy and sample entropy. Am J Physiol Heart Circ Physiol 2000;278:H2039–H2049.
40. Lord B, Allen JJB. Evaluating EEG complexity metrics as biomarkers for depression. Psychophysiology 2023;60:e14274.
41. Sorrentino A, Signore S, Qanud K, et al. Myocyte repolarization modulates myocardial function in aging dogs. Am J Physiol Heart Circ Physiol 2016;310:H873–H890.
42. Borghetti G, Eisenberg CA, Signore S, et al. Notch signaling modulates the electrical behavior of cardiomyocytes. Am J Physiol Heart Circ Physiol 2018;314:H68–H81.
43. Goldberger AL, Amaral LA, Glass L, et al. PhysioBank, PhysioToolkit, and PhysioNet: components of a new research resource for complex physiologic signals. Circulation 2000;101:E215–E220.
44. Schumann A, Bär KJ. Autonomic aging—a dataset to quantify changes of cardiovascular autonomic function during healthy aging. Sci Data 2022;9:95.
45. Schumann A, Bär K. Autonomic aging: a dataset to quantify changes of cardiovascular autonomic function during healthy aging (version 1.0.0). PhysioNet 2021; https://doi.org/10.13026/2hsy-t491. RRID:SCR_007345.
46. Rousselet GA, Pernet CR, Wilcox RR. Beyond differences in means: robust graphical methods to compare two groups in neuroscience. Eur J Neurosci 2017;46:1738–1748.
47. Benjamini Y, Hochberg Y. Controlling the false discovery rate: a practical and powerful approach to multiple testing. J R Stat Soc Ser B Stat Methodol 1995;57:289–300.
48. Maris E, Oostenveld R. Nonparametric statistical testing of EEG- and MEG-data. J Neurosci Methods 2007;164:177–190.
49. Ecker PM, Lin CC, Powers J, Kobilka BK, Dubin AM, Bernstein D. Effect of targeted deletions of β_1- and β_2-adrenergic-receptor subtypes on heart rate variability. Am J Physiol Heart Circ Physiol 2006;290:H192–H199.
50. Calderon-Juarez M, Gonzalez-Gomez GH, Echeverria JC, Lerma C. Revisiting nonlinearity of heart rate variability in healthy aging. Sci Rep 2023;13:13185.
51. Tanindi A, Olgun H, Tuncel A, Celik B, Pasaoglu H, Boyaci B. Exercise electrocardiographic responses and serum cystatin C levels among metabolic syndrome patients without overt diabetes mellitus. Vasc Health Risk Manag 2011;7:59–65.

52. Kizilbash MA, Carnethon MR, Chan C, Jacobs DR, Sidney S, Liu K. The temporal relationship between heart rate recovery immediately after exercise and the metabolic syndrome: the CARDIA study. Eur Heart J 2006;27:1592–1596.
53. Deniz F, Katircibasi MT, Pamukcu B, Binici S, Sanisoglu SY. Association of metabolic syndrome with impaired heart rate recovery and low exercise capacity in young male adults. Clin Endocrinol (Oxf) 2007;66:218–223.
54. Gao M, Chen W, Gong ZK, Han L, Zhang L. Correlation between chronotropic incompetence and metabolic equivalents in patients with type 2 diabetes mellitus and concomitant metabolic syndrome. Panminerva Med 2015;57:115–119.
55. Cole CR, Blackstone EH, Pashkow FJ, Snader CE, Lauer MS. Heart-rate recovery immediately after exercise as a predictor of mortality. N Engl J Med 1999;341:1351–1357.
56. Lauer MS, Okin PM, Larson MG, Evans JC, Levy D. Impaired heart rate response to graded exercise: prognostic implications of chronotropic incompetence in the Framingham Heart Study. Circulation 1996;93:1520–1526.
57. Kitzman DW. Conventional wisdom in heart failure treatment challenged again: does heart rate lowering worsen exercise intolerance in heart failure with preserved ejection fraction? Circulation 2015;132:1687–1689.
58. Miller DJ, Sargent C, Roach GD. A validation of six wearable devices for estimating sleep, heart rate and heart rate variability in healthy adults. Sensors (Basel) 2022;22:6317.
59. Ferretti G, Licker MJ, Anchisi S, Moia C, Susta D, Morel DR. The effects of β_1-adrenergic blockade on cardiovascular oxygen flow in normoxic and hypoxic humans at exercise. Eur J Appl Physiol 2005;95:250–259.
60. Goldberger JJ, Challapalli S, Tung R, Parker MA, Kadish AH. Relationship of heart rate variability to parasympathetic effect. Circulation 2001;103:1977–1983.
61. Fontolliet T, Pichot V, Bringard A, et al. Testing the vagal withdrawal hypothesis during light exercise under autonomic blockade: a heart rate variability study. J Appl Physiol (1985) 2018;125:1804–1811.
62. Nwazue VC, Paranjape SY, Black BK, et al. Postural tachycardia syndrome and inappropriate sinus tachycardia: role of autonomic modulation and sinus node automaticity. J Am Heart Assoc 2014;3:e000700.
63. Sethi KK, Jaishankar S, Balachander J, Bahl VK, Gupta MP. Sinus node function after autonomic blockade in normals and in sick sinus syndrome. Int J Cardiol 1984;5:707–719.
64. Michael S, Graham KS, Davis GMO. Cardiac autonomic responses during exercise and post-exercise recovery using heart rate variability and systolic time intervals—a review. Front Physiol 2017;8:301.
65. Stewart JM, Medow MS. Can standing replace upright tilt table testing in the diagnosis of postural tachycardia syndrome (POTS) in the young? Clin Auton Res 2025;35:257–266.
66. Lambert GW, Straznicky NE, Lambert EA, Dixon JB, Schlaich MP. Sympathetic nervous activation in obesity and the metabolic syndrome—causes, consequences and therapeutic implications. Pharmacol Ther 2010;126:159–172.
67. Czernichow S, Greenfield JR, Galan P, et al. Macrovascular and microvascular dysfunction in the metabolic syndrome. Hypertens Res 2010; 33:293–297.
68. Tune JD, Goodwill AG, Sassoon DJ, Mather KJ. Cardiovascular consequences of metabolic syndrome. Transl Res 2017;183:57–70.
69. Kaplan A, El-Samadi L, Zahreddine R, Amin G, Booz GW, Zouein FA. Canonical or non-canonical, all aspects of G protein-coupled receptor kinase 2 in heart failure. Acta Physiol (Oxf) 2025;241:e70010.
70. Signore S, Sorrentino A, Ferreira-Martins J, et al. Inositol 1,4,5-trisphosphate receptors and human left ventricular myocytes. Circulation 2013; 128:1286–1297.
71. Shinlapawittayatorn K, Pongkan W, Sivasinprasasn S, Chattipakorn SC, Chattipakorn N. Sexual dimorphism in cardiometabolic and cardiac mitochondrial function in obese rats following sex hormone deprivation. Nutr Diabetes 2022;12:11.
72. Ortiz-Guzman JE, Molla-Casanova S, Serra-Ano P, et al. Short-term heart rate variability in metabolic syndrome: a systematic review and meta-analysis. J Clin Med 2023;12:6051.
73. Ortiz-Guzman JE, Molla-Casanova S, Arias-Mutis OJ, et al. Differences in long-term heart rate variability between subjects with and without metabolic syndrome: a systematic review and meta-analysis. J Cardiovasc Dev Dis 2023; 10:203.
74. Stuckey MI, Tulppo MP, Kiviniemi AM, Petrella RJ. Heart rate variability and the metabolic syndrome: a systematic review of the literature. Diabetes Metab Res Rev 2014;30:784–793.
75. Zanoli L, Empana JP, Estrugo N, et al. The neural baroreflex pathway in subjects with metabolic syndrome: a sub-study of the Paris Prospective Study III. Medicine (Baltimore) 2016;95:e2472.
76. Goldberger AL, Amaral LA, Hausdorff JM, Ivanov P, Peng CK, Stanley HE. Fractal dynamics in physiology: alterations with disease and aging. Proc Natl Acad Sci U S A 2002;99:2466–2472.
77. Agliari E, Barra A, Barra OA, Fachechi A, Franceschi Vento L, Moretti L. Detecting cardiac pathologies via machine learning on heart-rate variability time series and related markers. Sci Rep 2020;10:8845.
78. Rajendra Acharya U, Faust O, Adib Kadri N, Suri JS, Yu W. Automated identification of normal and diabetes heart rate signals using nonlinear measures. Comput Biol Med 2013;43:1523–1529.
79. Zamora-Justo JA, Campos-Aguilar M, Beas-Jara MDC, et al. Utility of nonlinear analysis of heart rate variability in early detection of metabolic syndrome. Front Physiol 2025;16:1597314.
80. Fengade VS, Swati H, Chandak M, et al. Development of enhanced machine learning models for predicting type 2 diabetes mellitus using heart rate variability: a retrospective study. Cureus 2025;17:e80933.